





Article

Potassium Sulfate: A New Candidate to Explore Non-Photochemical Laser-Induced Nucleation Mechanisms

Mélody Briard ¹, Clément Brandel ^{1,*} , Sandrine Morin-Grognon ² , Gérard Coquerel ¹  and Valérie Dupray ¹ 

¹ Laboratoire Sciences et Méthodes Séparatives, Université de Rouen-Normandie, Normandie Université, 76000 Rouen, France; melody.briard@univ-rouen.fr (M.B.); gerard.coquerel@univ-rouen.fr (G.C.); valerie.dupray@univ-rouen.fr (V.D.)

² Polymères, Biopolymères, Surfaces, Université de Rouen-Normandie, Normandie Université, INSA Rouen, Centre National de la Recherche Scientifique, 55 rue Saint-Germain, 27000 Évreux, France; Sandrine.morin@univ-rouen.fr

* Correspondence: clement.brandel@univ-rouen.fr

Abstract: In this paper, we report a study on the nucleation behavior of potassium sulfate (K_2SO_4) from aqueous solutions under the influence of unfocused nanosecond laser pulses. The objective is to contribute to the general understanding of the Non-Photochemical Laser-Induced Nucleation (NPLIN) mechanism. First, the influence of several parameters such as supersaturation as well as laser parameters (pulse energy, number of pulses, and laser polarization) on induction time, probability of nucleation and mean number of crystals in comparison with spontaneous nucleation was investigated. Then, we examined the influence of gas composition (i.e., degassing and gas bubbling (CO_2 and N_2)) of the supersaturated solutions on the NPLIN kinetics, showing no correlation between gas content (or nature) on the crystallization behavior. Our study questions the role of impurities within the solution regarding the mechanism of laser-induced nucleation.

Keywords: NPLIN; pulsed laser; nucleation; potassium sulfate; cavitation mechanism



Citation: Briard, M.; Brandel, C.; Morin-Grognon, S.; Coquerel, G.; Dupray, V. Potassium Sulfate: A New Candidate to Explore Non-Photochemical Laser-Induced Nucleation Mechanisms. *Crystals* **2021**, *11*, 1571. <https://doi.org/10.3390/cryst11121571>

Academic Editor: Hao-chung Kuo

Received: 23 November 2021

Accepted: 13 December 2021

Published: 16 December 2021

Publisher's Note: MDPI stays neutral with regard to jurisdictional claims in published maps and institutional affiliations.



Copyright: © 2021 by the authors. Licensee MDPI, Basel, Switzerland. This article is an open access article distributed under the terms and conditions of the Creative Commons Attribution (CC BY) license (<https://creativecommons.org/licenses/by/4.0/>).

1. Introduction

Non-photochemical laser-induced nucleation (NPLIN) is a crystallization phenomenon discovered by Garetz et al. in 1996 [1] while performing second harmonic generation experiments on supersaturated urea solutions. They showed that high-energy laser delivering very short (i.e., <100 ns) light pulses can induce crystal nucleation from supersaturated solutions. The term “non-photochemical” excludes any photochemical reaction, implying that neither the solute nor the solvent absorbs at the wavelength used. Thus far, NPLIN phenomena have been reported for a number of compounds, mainly small organic molecules [1–5], but also salts with a majority of halides [6–8] and some cases of nitrates [9] and sulfates [10], as well as some proteins [11–13].

Several mechanisms were proposed to explain the NPLIN phenomenon. The first results and observations by Garetz et al. were explained by means of the optical Kerr effect (OKE): because of their anisotropic polarizability, the solvated molecules interact with the electromagnetic field of the laser light, which results in an alignment of the dipoles. The cooperativity of this event occurring in pre-nucleation clusters results in crystal nucleation. Garetz et al. also invoked the OKE mechanism to explain the polymorphic control of glycine by changing the polarization geometry of the laser light [2]. Indeed, they claimed that linear polarization was more effective at aligning dipoles with rod-like polarizabilities, thus resulting in the crystallization of γ -glycine, whereas circular polarization was more effective at aligning dipoles with disk-like polarizabilities, thus resulting in the crystallization of α -glycine. Several NPLIN cases have been claimed to rely on the OKE ever since [3,14–16], but several researchers have questioned the systematic implication of this phenomenon. First, it appears that the polarization dependence of glycine polymorphism during NPLIN

could not be reproduced [17–19]. Liu et al. [20] measured the relative angle between urea crystals and the electromagnetic field and showed that there is no alignment of the crystal with the direction of polarization of the laser, contrary to Garetz's first observations [1]. In addition, Monte Carlo simulations [21] of molecular orientations in the presence of an electromagnetic field showed that if an orientational bias can indeed reduce the free energy barrier for nucleation, the required electromagnetic field should be several times higher than that used in typical NPLIN experiments (e.g., for glycine the orientational bias parameter is 10^{-5} , whereas it must be closed to 10^{-1} to have an effect). Further to this, the OKE is hardly conceivable for NPLIN phenomena when the compound of interest crystallizes in a cubic space group (similar to many simple organic salts). Alexander and Camp [6] reported and discussed NPLIN experiments on aqueous supersaturated potassium chloride (KCl) solutions. They have shown that there is no dependence of the nucleation kinetics on polarization and proposed that NPLIN of KCl is based on a dielectric polarization (DP) phenomenon, which reduces the free energy required to nucleate in the presence of the laser electromagnetic field.

Another possible mechanism envisaged for NPLIN is that crystallization is related to the nucleation and/or behavior under laser irradiation of gaseous matter present in the supersaturated solution. This hypothesis has been proposed by Knott et al. [22]. They have shown that laser pulses can interact with dissolved gas since they triggered the nucleation and growth of macroscopic CO₂ bubbles from a carbonated aqueous solution supersaturated with this gas.

As discussed by the authors, OKE and DP mechanisms are obviously not valid hypotheses in this situation. Rather, the laser pulses would interact with impurity particles in the solution, resulting in transient and local heating of the system [23], leading eventually to gas nucleation. These gas bubbles can be visible and stable, but there is evidence that laser pulses can also give rise to short-lived and very small gaseous cavities.

Knott et al. [22] have also shown that the nucleation of gas is correlated to crystal nucleation, in solution supersaturated with both argon and glycine, the presence of argon bubble induced the crystallization of glycine. The formation of a gas bubble can act as a heterogeneous surface for crystal nucleation or trigger crystallization upon its collapse due to the emission of a pressure wave. NPLIN would not be the direct consequence of an interaction between the laser light and the solvated molecule but a collateral effect of gas nucleation. This is further supported by a study of Javid et al. [24], who have shown that NPLIN of glycine can be suppressed by careful “nanofiltration” of the aqueous solutions: it highlights that removing dust and small impurities from the solutions hampers crystal nucleation [7,24,25], most likely due to the absence of bubble formation. Another supporting evidence to such mechanism is the study by Mirsaleh-Kohan et al. [26], who have shown that crystal nucleation of a supersaturated solution can be triggered by focusing the laser beam on a metal plate floating on the top of the solution: focused laser pulses would produce shock waves that induce crystallization. Such pressure waves can be compared with those produced by the collapse of gas cavities, which would mean that NPLIN is only due to that mechanical effect. Yet, Kacker et al. [27] described a similar experiment during which an unfocused laser beam failed to trigger nucleation if the glass vials were masked with black tape, whereas NPLIN occurred normally in unmasked vials. It has also recently been demonstrated that pressure waves generated by the irradiation of different materials with 1064 nm nanosecond laser pulses can influence drug delivery [28].

There is no general consensus regarding the NPLIN mechanism, and the data collected and published since 1996 suggest diverse behaviors from one compound to another. More experiments and more case studies are therefore needed to further understand how laser pulses can interact with the supersaturated solution to induce crystallization.

In this publication, we report a new case of NPLIN applied to an inorganic salt. The NPLIN of potassium sulfate supersaturated solutions was triggered by using nanosecond pulses of an unfocused high-energy Nd: YAG laser. Among several tested salts, potassium sulfate was chosen because of the following properties: it exhibits (i) a noncubic space

group (P_{nam} (62) [29]); (ii) no polymorph or hydrate under our experimental conditions (one polymorph exists above 580 °C [30]); (iii) crystallization kinetics (spontaneous and NPLIN) measurable on a laboratory scale; (iv) an appropriate solubility in water (sufficient to observe the crystallization and not too large to control it); (v) a very low absorption at 1064 nm (absorbance for a saturated solution of K_2SO_4 in water is 0.058 cm^{-1}).

A systematic approach is developed in order to identify the incidence of both the laser parameters and the solution supersaturation on the nucleation behavior. Moreover, the influence of gases dissolved in solution on the NPLIN behavior is examined in order to study the role of gas nucleation on crystallization.

2. Materials and Methods

2.1. Preparation of the Metastable Solutions of K_2SO_4 in Water

Potassium sulfate (K_2SO_4), with a purity of 99%, was purchased from MERCK (Germany) and was used without further purification. Water was demineralized ($2\text{--}8\text{ }\mu\text{S}\cdot\text{cm}^{-1}$) with an osmosis unit water purification system from OSMOTECH (Buchelay, France). The solubility of K_2SO_4 in water was measured at 20 °C by the gravimetric method, and a value of $S = 10.05\%$ wt was obtained. This value was compared with literature data; Mydlarz and Jones [31] reported solubility values of different references expressed in kg of K_2SO_4 /kg of water, converting into weight percentage, and values ranged from 9.83%wt and 10.06%wt; thus, our value appeared to be in good agreement with the one of Mydlarz et al. [32]. The supersaturation domain investigated ranged from $\beta = 1.15$ to 1.25 (β is the supersaturation ratio and is defined as C/S , with C , the solution concentration) at a constant temperature of 20 °C. For the preparation of the solutions to be irradiated, a large volume of solution was prepared and heated until complete dissolution. Then, the stock solution was transferred in at least 50 glass vials (dimensions: 1.2 cm diameter, 1 mm thickness, total height 2.6 cm) using a precision pipette (VWR EHP 100–1000 μL) set at 1 mL. After each transfer, each vial was carefully closed with a screw cap equipped with a rubber seal to avoid evaporation. The pipette tip was also changed every 5 vials to avoid solvent evaporation and undesired solution seeding. Then, all the vials were placed in an oven at 50 °C for at least 3 h in order to ensure total dissolution of the solute and avoid uncontrolled crystallization. It was confirmed that no solvent evaporation occurred during this step. Then, the vials were placed in a thermostated room at 20 °C for at least 1 h before irradiation.

2.2. NPLIN Setup

A Q-switched Nd-YAG laser NL300 (EKSPLA, Vilnius, Lithuania distributed by Opton Laser, Orsay, France) emitting at wavelength 1064 nm, with a pulse width of 5.3 ns (τ), a beam diameter of 6 mm, and a pulse repetition frequency of 10 Hz (ν) was used. A quarter-wave plate was placed on the beam path to control its polarization geometry, from linear to either right or left circularly polarized light. Figure 1 shows a picture of the experimental setup. The pulse energy was measured by means of a power meter NOVA II with a pyroelectric sensor (PE50BF-DIFH-C (OPHIR, Jerusalem, Israel distributed by MKS, Virigneux, France); we applied pulse energy (E_p) varying from 18 to 85.6 mJ (value without vial on the beam path), which corresponds to laser peak intensity ranging from 12 to 58 $\text{MW}\cdot\text{cm}^{-2}$, that is to say, in the same order of magnitude as for experiments performed using other inorganic salts [6,27]. A reduction in the laser intensity entering the solution must be considered, which is mainly due to the reflection occurring at the vial surface (the absorption coefficient of silica glasses is almost negligible at the working wavelength). This reduction is estimated at circa 4%, considering the indexes of refraction of both the air and the glass ($n_{\text{air}} = 1.0003$; $n_{\text{glass}} = 1.5066$ [33]). Note that, the values of energy given herein did not include the 4% reduction. The irradiated volume could be compared with the volume of a truncated cone due to the focalization of the beam. At the exit of the vial, the beam had an elliptical shape with $3 \times 6\text{ mm}$ dimensions. Thus, we estimated the irradiated volume to be circa 0.20 mL, considering the solution as static. As we used a 1 mL solution, only

20% of the solution was irradiated. It is also of note that the laser and the optical table were all stored in a dark and air-conditioned room at 20 °C.

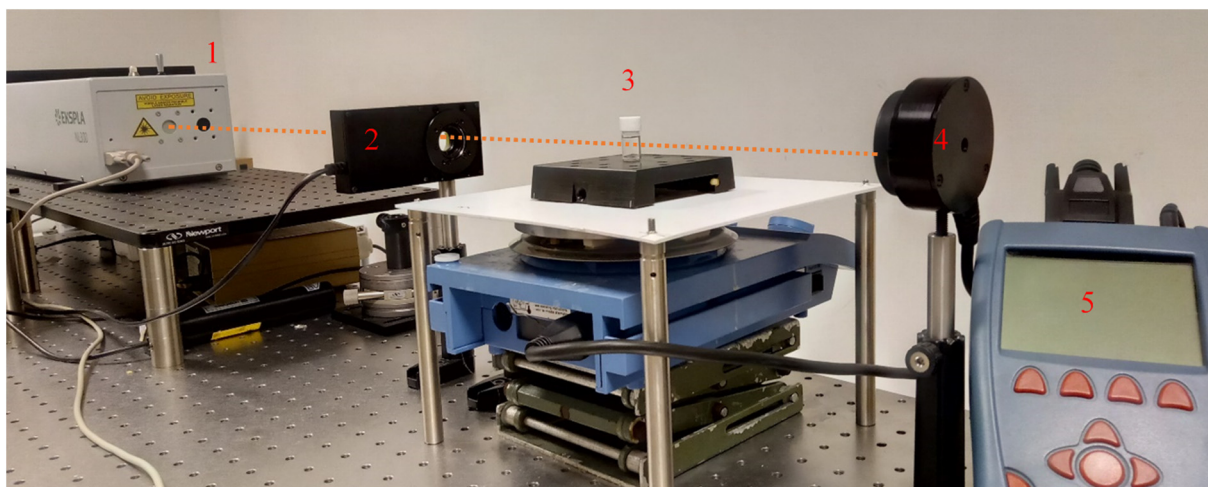


Figure 1. Experimental setup used for NPLIN experiments: 1—laser; 2—quarter-wave plate; 3—sample; 4—sensor; 5—power meter.

2.3. NPLIN Experiments

For a given set of samples, irradiation was carried out for ca. 75% of the vials. The remaining 25% were not illuminated and served as blank experiments. We used a number of pulses ranging from 1 to 100, with pulse energy varying from 18 to 85.6 mJ (incident light). The crystallization progress was estimated through 3 factors:

The first factor was the induction time t_i , which is the time between laser exposure and the observed onset of nucleation. This duration was monitored by regular inspection of the vials. Obviously, this is a rough estimation of the induction time, as small nuclei are not immediately visible to the naked eye.

The second factor was the probability of nucleation $P_n(t)$ [34], i.e., the number of crystallized vials after a time t ($N_{cryst}(t)$) over the total number of irradiated vials (N_{vials}) (Equation (1)). Indeed, because of the stochasticity of nucleation, each vial will nucleate differently.

$$P_n(t) = \left(\frac{N_{cryst}(t)}{N_{vials}} \right) \times 100 \quad (1)$$

The third factor was the mean number of crystals per vial for the different experiments. The crystal morphology was also controlled by optical microscopy.

2.4. Preparation of the K_2SO_4 Solutions Saturated with Different Gas

To study the influence of dissolved gas on the NPLIN behavior of K_2SO_4 , the above protocol was applied with the following modification. First, water was sonicated in an ultrasonic bath (VWR USC100T, 45KHz, 30W) for five minutes for degassing, then an adequate amount of K_2SO_4 was added and the vessel containing the stock solution was rapidly sealed. While heating the stock solution, the selected gas was bubbled into the solution by using a gas-filled balloon connected to a needle for at least 30 min. Nitrogen gas was purchased from Air liquide (France) with a purity of 99.9999% (Alphagaz2). Carbon dioxide was produced by a chemical reaction between calcium carbonate (RP Normapur 99%) and hydrochloric acid 37%, purchased from VWR Chemicals. The remainder of the experiment was similar to a regular NPLIN experiment, although extra care was taken in order to prevent uncontrolled gas departure from solutions.

3. Results and Discussion

3.1. Influence of Supersaturation on the Nucleation Kinetics and the Probability of Nucleation

To study the influence of supersaturation on the NPLIN kinetic of K_2SO_4 at 20 °C, vials containing the metastable solution of K_2SO_4 at supersaturation of $\beta = 1.25$, 1.2, and 1.15 (at least 50 individuals in each case) were exposed to one laser pulse with a pulse energy of 18 mJ at the entrance of the vial. The number of pulses was limited to a single shot in order to minimize the heating effect due to the water absorption at 1064 nm (At this wavelength the absorption coefficient is 0.1 cm^{-1} [15]). By using atomic force microscopy and scanning electron microscopy, we ensured that the structure of the glass was not damaged by irradiation: The surface aspect of the inner side of the vials was found to be similar before and after irradiation, and the formation of shattered glass particles was unlikely (Figures S1 and S2 and Table S1). To compare the kinetics of spontaneous crystallization with that of NPLIN experiments, control samples (at least 10 individuals for each value of β) were prepared with the same procedure and were not exposed to laser light. The results are presented in Figure 2.

Nanosecond pulsed nIR irradiation favors nucleation. Indeed, Figure 2 clearly shows that laser irradiation allowed a decrease in the induction time in a significant number of samples since; for example, 24 h after irradiation, the probability of nucleation more than doubled, compared with unexposed samples. This is a clear manifestation of the NPLIN phenomenon, and it must be underlined that such behavior was not systematically observed in every compound that was investigated. As expected, Figure 2 highlights that the control of supersaturation is as important a parameter in the NPLIN process as in any nucleation process: the higher the supersaturation is, the more labile to nucleation the system. However, if the probability of nucleation of irradiated and control samples both reached 100% (although at different rates) when $\beta = 1.25$, it is also worth noting that the curves obtained at lower supersaturations both converged to the same value of the probability of nucleation, and after circa 72 h, a probability of nucleation of 100% was reached regardless of the supersaturation. This suggests that the nucleation of K_2SO_4 could have two kinds of regime—one that is sensitive to irradiation and one that is not.

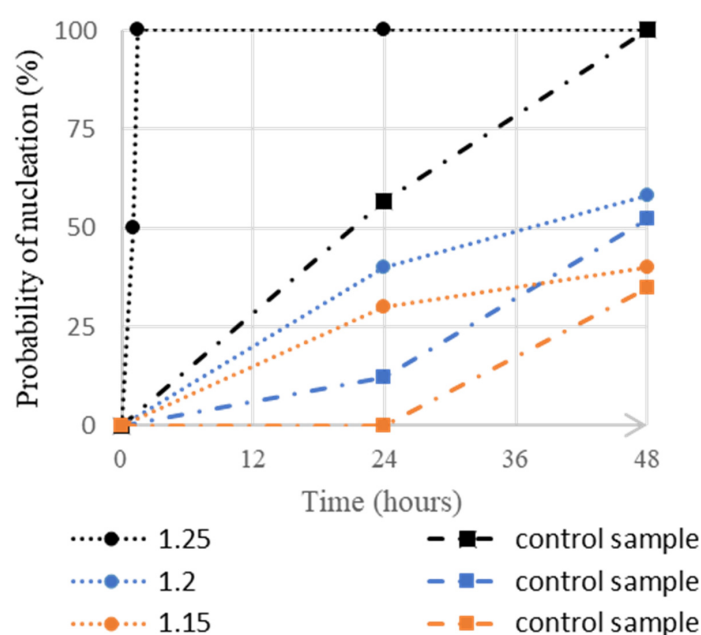


Figure 2. Evolution of the experimental probability of nucleation after laser irradiation over time (in hours) for different supersaturations: (a) $\beta = 1.25$; (b) $\beta = 1.20$; (c) $\beta = 1.15$. All samples were exposed to 1 pulse at 18 mJ ($12\text{ MW}\cdot\text{cm}^{-2}$) (circles ●). Control samples were not exposed to laser; they nucleated spontaneously (squares ■). The dashed lines guide the eyes.

It is worth mentioning that no difference in the number of crystals was detected when changing the supersaturation. The mean number of crystals per vial was observed to be circa 1.5, usually obtaining 1–2 crystals for each irradiated sample, with some cases up to 4 crystals. For control samples, the value was closer to 1.3. Careful observations of the crystals produced either by spontaneous crystallization or by laser pulses showed constant crystal morphologies, various crystal shapes, and the occasional occurrence of twinned crystals in both cases (Figure 3).



Figure 3. K₂SO₄ crystals obtained from supersaturated solutions $\beta = 1.25$: typical twin crystals observed in this study (left), crystals obtained by laser irradiation (middle), and crystals obtained by spontaneous nucleation (right). Pictures were taken with a NIKON SMZ-10A microscope equipped with a Sony DXC-950 3CCD Color Video Camera Power HAD.

3.2. Influence of the Number of Pulses and Intensity

Supersaturation was fixed at $\beta = 1.25$ to study the influence of the number of pulses, as well as their intensity on the NPLIN kinetics and on the number of produced K₂SO₄ crystals. Table 1 shows the changes in induction time, probability of nucleation, and the number of crystals produced. First, at constant laser intensity, there was a slight increase in the probability of nucleation upon increasing the number of pulses from 1 to 100. Second, when increasing the laser intensity from 18 to 85.6 mJ, the induction time was reduced by half. This result is in agreement with several studies [5,6,15,35], particularly that by Kacker et al. [27], who stated that the nucleation probability depends on the laser beam intensity. Furthermore, there was an increase in the number of crystals produced, which is actually dependent on both the number of pulses and the intensity of the laser. Alexander et al. [6] found that a single laser pulse can yield a single crystal of potassium chloride. Although we observed that a single pulse of 18 mJ is likely to induce the nucleation of an isolated crystal of K₂SO₄, it seems that the use of higher energy generates more crystals. This is in line with the observation of Hua et al. [35], who found that the number of crystal nucleated is proportional to the laser intensity. Yet, it should be underlined that Irimia et al. [19] showed that the nucleation probability of glycine aqueous solutions actually decreases when more than 600 pulses are used due to the overall temperature increase (and associated supersaturation decrease) of the solution. For our study, the temperature increase was calculated for our experimental conditions (1 pulse at 85.6 mJ, $\beta = 1.25$) using the same theoretical model developed and experimentally validated by Irimia et al. The calculated C_p value of $3.75 \text{ J g}^{-1} \text{ K}^{-1}$ led to an overall increase in temperature (in the area illuminated by the laser) of $2.4 \times 10^{-3} \text{ K/pulse}$, which was not sufficient to change the overall supersaturation of the solutions.

Table 1. Influence of the number of pulse and its intensity on the nucleation behavior of K₂SO₄ solutions at $\beta = 1.25$. Np is the number of pulses; Ep is the intensity or pulse energy.

Np	Ep (mJ)	Induction Time (min)	Probability of Nucleation (%) (t = 1.5 h)	Number of Crystals Per Vial (min–max)
1	18	60	40	1–4
101	18	60	80	1–8
1	85.6	30	100	3–6
101	85.6	30	100	>30

3.3. Influence of the Laser Polarization

In their study on KCl, Alexander et al. [6] showed that there is no influence of the polarization of the laser on nucleation. To confirm this statement, the influence of polarization on the NPLIN kinetics of K₂SO₄ solution was investigated by using a supersaturation ratio of $\beta = 1.25$. Solutions were irradiated with one pulse at 85.6 mJ by using either linear or circular polarized light. As can be seen in Table 2, no difference was observed between the two polarizations in terms of induction time, probability of nucleation, the number of crystals, or visual aspects of crystals and nucleation kinetics.

Table 2. Influence of the type of polarization on the nucleation behavior of K₂SO₄ solutions at $\beta = 1.25$: LP (linear polarization), RCP (right circular polarization), and LCP (left circular polarization).

Polarization	Induction Time (min)	Probability of Nucleation % (t = 1.5 h)	Number of Crystals Per Vial (min–max)
LP	30	100	3–6
RCP	30	100	2–6
LCP	30	100	2–7

According to the OKE mechanism, the use of the appropriate polarization (linear, circular, or elliptical) should result in an increase in the probability of nucleation and in a reduction in the induction time. For example, Matic et al. [15] found that the probability of NPLIN is higher with linear polarization than circular polarization for solutions of urea. There are, however, reported cases, such as Alexander and Camp [6], showing that the induction time is not correlated to polarization geometry. In the case of glycine, Garetz et al. [2,16] have shown that, for a range of supersaturation, the geometry of polarization induces different polymorphs, which was considered in this study as an argument in favor of the OKE model (although this experiment could not be reproduced) [17,19].

K₂SO₄ exhibits two polymorphs—the β form (*Pnam* (62)) [29], which is stable up to 583 °C but transforms into the α form at a higher temperature (*P6₃/mmc*) [30]. In our experiments, only the β form was observed regardless of the polarization and supersaturation used, and no trace of any hydrated form was detected. The hypothesis that the occurrence of an OKE would be possible provided pre-nucleation clusters exhibited a structure similar to the final crystals (indeed, such an orthorhombic structure should exhibit birefringence) was not confirmed by the results shown in Table 2. Indeed, values from the literature [36] revealed very weak birefringence, indicating that there is no strong polarization axis in the crystalline structure. As a consequence, it was confirmed that there was no evidence of OKE occurring during our experiments. This prompted us to investigate the role of gaseous matter in the mechanism of NPLIN of K₂SO₄.

3.4. Influence of Gas Composition and Nature

Knott et al. [22] reported that the irradiation of a solution supersaturated with CO₂ results in the nucleation of stable CO₂ gas bubbles. They also suggested that gas nucleation could play a role in the NPLIN of crystals since they observed that a solution co-supersaturated with argon and glycine, after gentle shaking, first nucleates gas bubbles and then glycine crystals. Although valuable, these experiments have been performed in experimental conditions that differ from the actual conditions used during regular NPLIN experiments: dissolved gas is likely not supersaturated. Although this might reduce the

probability of nucleation of gaseous bubbles, gas nucleation can still be envisaged even when the gas content of a solution is below its saturation: The presence of dissolved nanoparticles (such as inorganic impurities) can result in the absorption of the laser energy and induce temperature increase [7,25]. Such local solution heating can possibly result in (i) local vaporization of the solution and nucleation of vapor bubbles (gas bubbles would consist of vaporized solution); (ii) nucleation of gaseous matter (gases exhibit retrograde solubility) due to a significant solubility decrease (gas bubbles would consist of CO₂, N₂, O₂, or air); (iii) a combination of (i) and (ii) in which vapor bubbles act as seeds for the nucleation of other gas bubbles, as suggested by Ward et al. [25]. In the three mentioned situations, the formation of gaseous bubbles ultimately results in their collapse, followed by crystal nucleation.

In order to discriminate between (i), (ii), and (iii) in the case of K₂SO₄ aqueous solutions, a supplementary set of NPLIN experiments was performed by evaluating the incidence of an experimental parameter that has only been scarcely considered in other publications—controlled gas composition. Indeed, there is, to the best of our knowledge, no study focusing on the kinetics of NPLIN as a function of the presence of dissolved gas in the supersaturated solution, both in terms of nature and composition.

We designed an experiment aiming at evaluating the NPLIN kinetics and nucleation probability of K₂SO₄ solutions as a function of the controlled presence of several dissolved gas. To that end, supersaturated solutions ($\beta = 1.25$) of K₂SO₄ were saturated with gas by bubbling (air, N₂, or CO₂, see Section 2) or degassed by exposition to ultrasounds before systematic laser irradiation. Provided hypothesis (ii) was valid, different dissolved gas should have exhibited different gas nucleation behaviors upon laser irradiation, which should have, in turn, resulted in significantly different crystal nucleation behaviors. It is also worth mentioning that a marked drop in the nucleation probability was expected if the supersaturated solutions were degassed prior to irradiation.

The crystal nucleation probability of the irradiated solutions as a function of time and gas composition is shown in Figure 4. For each gas condition, at least 100 vials were exposed to one single pulse at 85.6 mJ. The laser energy value was chosen to stay in the same order of magnitude as in the two publications dedicated to the nucleation of gaseous bubbles [22,25] (unfocused nanosecond laser pulses).

It should first be underlined that no macroscopic gas bubbles were observed during these experiments and that, if that occurred, the formed cavities were too small and/or short lived. Figure 4 shows that, although the presence of N₂ and CO₂ seems to slightly reduce the induction time, the four $P_n(t) = f(t)$ curves remained quite similar: The kinetics of NPLIN of K₂SO₄ seems uncorrelated to the presence (or the absence) of dissolved gas, regardless of the nature of the gas tested. In particular, the fact that CO₂- and N₂-saturated solutions gave the same NPLIN kinetics is valuable information. Indeed, the solubility of these two gases in water is considerably different [37]; thus, laser irradiation should produce significantly different amounts of gas cavities, and notable differences of NPLIN kinetics should have been observed for K₂SO₄. Degassed solutions also exhibited a similar NPLIN regime to gas bubbled samples. Therefore, hypothesis (i) involving local heating and solution vaporization seemed more likely.

Concerning the nature of the interacting impurities, several hypotheses can be considered: The impurities could be gaseous bubbles already present in the solution before irradiation, even in the case of degassed solution (a recent study from Lee et al. [38] estimates that the number of gas bubbles in degassed deionized water is of circa 4×10^7 per mL with a mean diameter of circa 250 nm). However, the absorption coefficient of gases at 1064 nm was very low, and it was unlikely that light absorption by the gaseous bubble could induce sufficient local heating of the solution. Impurities could also be solid nanoparticles present in the solution, as suggested by various authors, and this could explain the energy threshold often observed in NPLIN experiments: Ward et al. [25] indeed showed, in a theoretical study, that presence of nanoparticles of graphite or iron oxide in the solution could result in the nucleation of gaseous bubbles. However, the question remains that if NPLIN is correlated to

the presence of inorganic impurities, why does the wavelength of the laser have no incidence on the NPLIN kinetics? Solid nanoparticles indeed have different adsorption coefficients at different wavelengths, and the amount of heat transferred to the solution should be different when irradiated at 532 and 1064 nm.

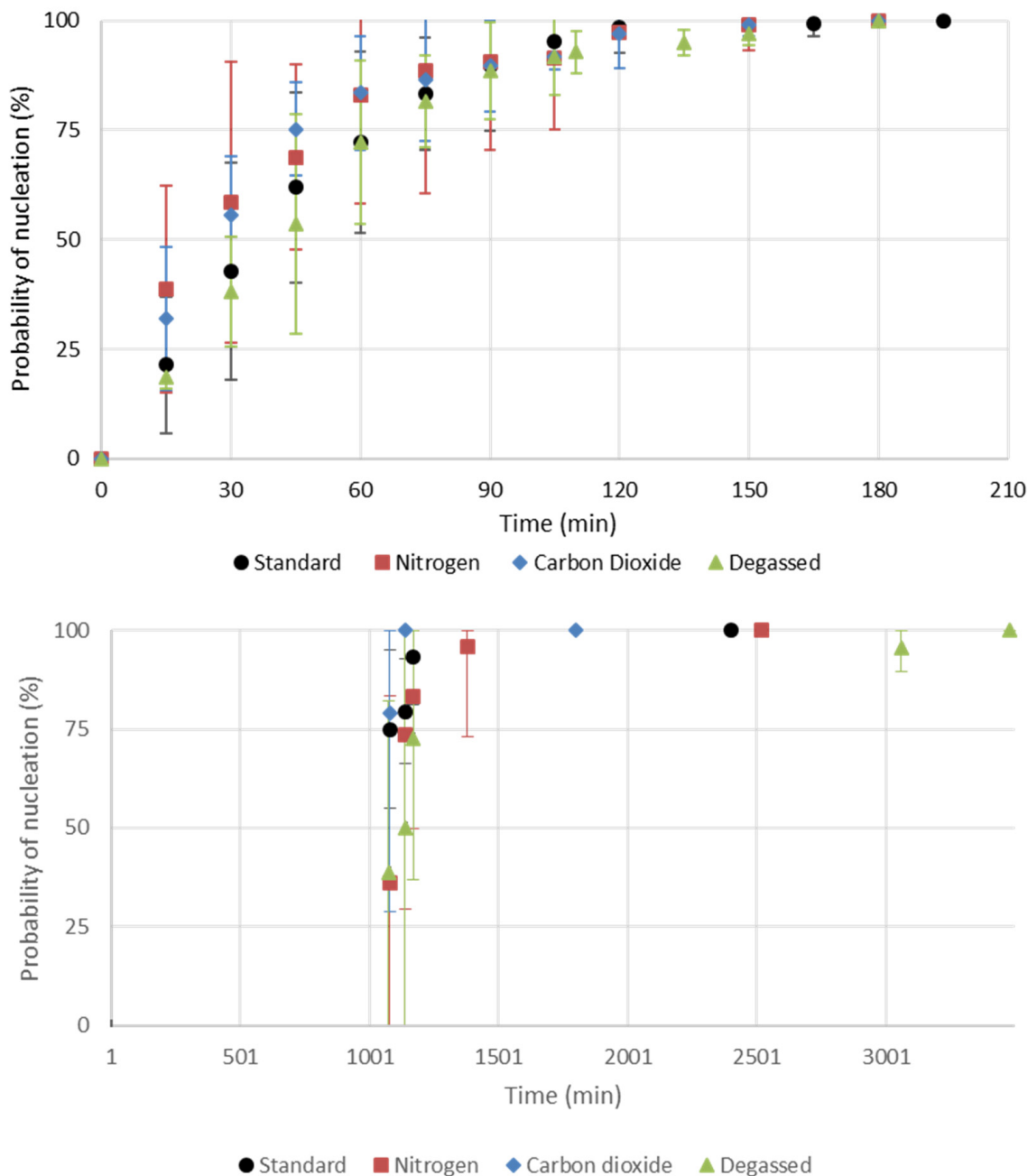


Figure 4. Influence of degassing and gas bubbling on the probability of NPLIN (**at the top**) and the probability of spontaneous nucleation (**at the bottom**) as a function of time (one pulse at 85.6 mJ). “Standard” stands for no solution treatment; “Nitrogen” and “Carbon Dioxide” are the gas used for bubbling; “Degassed” is solution degassed by ultrasounds.

4. Conclusions

This paper reported a new example of the non-photochemical laser-induced nucleation (NPLIN) phenomenon. We explored the influence of various experimental parameters on the NPLIN kinetics of K_2SO_4 metastable aqueous solutions, and, in particular, we used an original approach that consists of saturating the solution to be irradiated with two different gases with contrasted solubility in water in order to study the mechanisms of

cavitation and their connection with crystal nucleation upon laser irradiation. We showed that (i) higher pulse numbers and higher laser intensities significantly decrease induction time, but that nucleation kinetics of K_2SO_4 is (ii) not correlated to laser polarization and (iii) not correlated to the gas nature and content. These observations imply that no optical Kerr effect occurred in this study and that K_2SO_4 NPLIN is not a result of cavitation of dissolved gas. Although further experiments are required, it is likely that NPLIN rather occurs due to local and transient heating of the solutions, resulting in vapor bubbles, which collapse and trigger crystal nucleation via the propagation of a pressure wave. We conclude that future NPLIN experiments should focus on the impact of impurity content on the NPLIN kinetics.

Supplementary Materials: The following are available online at <https://www.mdpi.com/article/10.3390/cryst11121571/s1>, Figure S1: 3D representation of the inner surface roughness of the vial measured by atomic force microscopy (AFM): (a) a piece of control vial without any laser exposure; (b) and (c) a piece of vial exposed to 100 pulses at 85.6 mJ, respectively, the entry face and the exit face of the laser beam. The size of the surface analyzed is $25\ \mu\text{m} \times 25\ \mu\text{m}$, Figure S2: Scanning electron microscopy (SEM) images. From left to right: control vial, vial entry face, and vial exit face of the laser beam, Table S1: Roughness average (Ra) and maximum roughness (Rz) measured for control vial and irradiated vial (entry face and exit face of the laser beam).

Author Contributions: Conceptualization, C.B., V.D. and M.B.; methodology, M.B.; software, M.B.; validation, C.B., V.D. and M.B.; formal analysis, M.B. and S.M.-G.; investigation, M.B. and S.M.-G.; data curation, M.B. and S.M.-G.; writing—original draft preparation, M.B.; writing—review and editing, C.B., V.D., G.C. and M.B.; supervision, C.B. and V.D.; project administration, C.B., V.D. and G.C. All authors have read and agreed to the published version of the manuscript.

Funding: This research received no external funding.

Conflicts of Interest: The authors declare no conflict of interest.

References

- Garetz, B.A.; Aber, J.E.; Goddard, N.L.; Young, R.G.; Myerson, A.S. Nonphotochemical, Polarization-Dependent, Laser-Induced Nucleation in Supersaturated Aqueous Urea Solutions. *Phys. Rev. Lett.* **1996**, *77*, 3475. [CrossRef]
- Garetz, B.A.; Matic, J.; Myerson, A.S. Polarization Switching of Crystal Structure in the Nonphotochemical Light-Induced Nucleation of Supersaturated Aqueous Glycine Solutions. *Phys. Rev. Lett.* **2002**, *89*, 175501. [CrossRef]
- Sun, X.; Garetz, B.A.; Myerson, A.S. Polarization Switching of Crystal Structure in the Nonphotochemical Laser-Induced Nucleation of Supersaturated Aqueous L-Histidine. *Cryst. Growth Des.* **2008**, *8*, 1720–1722. [CrossRef]
- Wang, S.; Wang, S.; Jiang, L.; Wang, M.; Wei, Y.; Sun, J.; Zhan, S.; Li, X.; Qu, L. Polymorph-Controlled Crystallization of Acetaminophen through Femtosecond Laser Irradiation. *Cryst. Growth Des.* **2019**, *19*, 3265–3271. [CrossRef]
- Li, W.; Ikni, A.; Scoufflaire, P.; Shi, X.; El Hassan, N.; Gémeiner, P.; Gillet, J.-M.; Spasojević-de Biré, A. Non-Photochemical Laser-Induced Nucleation of Sulfathiazole in a Water/Ethanol Mixture. *Cryst. Growth Des.* **2016**, *16*, 2514–2526. [CrossRef]
- Alexander, A.J.; Camp, P.J. Single Pulse, Single Crystal Laser-Induced Nucleation of Potassium Chloride. *Cryst. Growth Des.* **2009**, *9*, 958–963. [CrossRef]
- Ward, M.R.; Mackenzie, A.M.; Alexander, A.J. Role of Impurity Nanoparticles in Laser-Induced Nucleation of Ammonium Chloride. *Cryst. Growth Des.* **2016**, *16*, 6790–6796. [CrossRef]
- Barber, E.R.; Kinney, N.L.H.; Alexander, A.J. Pulsed Laser-Induced Nucleation of Sodium Chlorate at High Energy Densities. *Cryst. Growth Des.* **2019**, *19*, 7106–7111. [CrossRef]
- Jacob, J.A.; Sorgues, S.; Dazzi, A.; Mostafavi, M.; Belloni, J. Homogeneous Nucleation-Growth Dynamics Induced by Single Laser Pulse in Supersaturated Solutions. *Cryst. Growth Des.* **2012**, *12*, 5980–5985. [CrossRef]
- Soare, A.; Dijkink, R.; Pascual, M.R.; Sun, C.; Cains, P.W.; Lohse, D.; Stankiewicz, A.I.; Kramer, H.J.M. Crystal Nucleation by Laser-Induced Cavitation. *Cryst. Growth Des.* **2011**, *11*, 2311–2316. [CrossRef]
- Lee, I.S.; Evans, J.M.B.; Erdemir, D.; Lee, A.Y.; Garetz, B.A.; Myerson, A.S. Nonphotochemical Laser Induced Nucleation of Hen Egg White Lysozyme Crystals. *Cryst. Growth Des.* **2008**, *8*, 4255–4261. [CrossRef]
- Yoshikawa, H.Y.; Murai, R.; Sugiyama, S.; Sazaki, G.; Kitatani, T.; Takahashi, Y.; Adachi, H.; Matsumura, H.; Murakami, S.; Inoue, T.; et al. Femtosecond Laser-Induced Nucleation of Protein in Agarose Gel. *J. Cryst. Growth* **2009**, *311*, 956–959. [CrossRef]
- Murai, R.; Yoshikawa, H.Y.; Hasenaka, H.; Takahashi, Y.; Maruyama, M.; Sugiyama, S.; Adachi, H.; Takano, K.; Matsumura, H.; Murakami, S.; et al. Influence of Energy and Wavelength on Femtosecond Laser-Induced Nucleation of Protein. *Chem. Phys. Lett.* **2011**, *510*, 139–142. [CrossRef]

14. Zaccaro, J.; Matic, J.; Myerson, A.S.; Garetz, B.A. Nonphotochemical, Laser-Induced Nucleation of Supersaturated Aqueous Glycine Produces Unexpected γ -Polymorph. *Cryst. Growth Des.* **2001**, *1*, 5–8. [CrossRef]
15. Matic, J.; Sun, X.; Garetz, B.A.; Myerson, A.S. Intensity, Wavelength, and Polarization Dependence of Nonphotochemical Laser-Induced Nucleation in Supersaturated Aqueous Urea Solutions. *Cryst. Growth Des.* **2005**, *5*, 1565–1567. [CrossRef]
16. Sun, X.; Garetz, B.A.; Myerson, A.S. Supersaturation and Polarization Dependence of Polymorph Control in the Nonphotochemical Laser-Induced Nucleation (NPLIN) of Aqueous Glycine Solutions. *Cryst. Growth Des.* **2006**, *6*, 684–689. [CrossRef]
17. Clair, B.; Ikni, A.; Li, W.; Scoufflaire, P.; Quemener, V.; Spasojević-de Biré, A. A New Experimental Setup for High-Throughput Controlled Non-Photochemical Laser-Induced Nucleation: Application to Glycine Crystallization. *J. Appl. Cryst.* **2014**, *47*, 1252–1260. [CrossRef]
18. Liu, Y.; van den Berg, M.H.; Alexander, A.J. Supersaturation Dependence of Glycine Polymorphism Using Laser-Induced Nucleation, Sonocrystallization and Nucleation by Mechanical Shock. *Phys. Chem. Chem. Phys.* **2017**, *19*, 19386–19392. [CrossRef]
19. Irimia, D.; Jose Shirley, J.; Garg, A.S.; Nijland, D.P.A.; van der Heijden, A.E.D.M.; Kramer, H.J.M.; Eral, H.B. Influence of Laser Parameters and Experimental Conditions on Nonphotochemical Laser-Induced Nucleation of Glycine Polymorphs. *Cryst. Growth Des.* **2020**, *21*, 631–641. [CrossRef]
20. Liu, Y.; Ward, M.R.; Alexander, A.J. Polarization Independence of Laser-Induced Nucleation in Supersaturated Aqueous Urea Solutions. *Phys. Chem. Chem. Phys.* **2017**, *19*, 3464–3467. [CrossRef]
21. Knott, B.C.; Doherty, M.F.; Peters, B. A Simulation Test of the Optical Kerr Mechanism for Laser-Induced Nucleation. *J. Chem. Phys.* **2011**, *134*, 154501. [CrossRef]
22. Knott, B.C.; LaRue, J.L.; Wodtke, A.M.; Doherty, M.F.; Peters, B. Communication: Bubbles, Crystals, and Laser-Induced Nucleation. *J. Chem. Phys.* **2011**, *134*, 171102. [CrossRef] [PubMed]
23. Rey-García, F.; Sieira, B.J.; Bao-Varela, C.; Leis, J.R.; Angurel, L.A.; Quintana, J.B.; Rodil, R.; de la Fuente, G.F. Can UV-C Laser Pulsed Irradiation Be Used for the Removal of Organic Micropollutants from Water? Case Study with Ibuprofen. *Sci. Total Environ.* **2020**, *742*, 140507. [CrossRef] [PubMed]
24. Javid, N.; Kendall, T.; Burns, I.S.; Sefcik, J. Filtration Suppresses Laser-Induced Nucleation of Glycine in Aqueous Solutions. *Cryst. Growth Des.* **2016**, *16*, 4196–4202. [CrossRef]
25. Ward, M.R.; Jamieson, W.J.; Leckey, C.A.; Alexander, A.J. Laser-Induced Nucleation of Carbon Dioxide Bubbles. *J. Chem. Phys.* **2015**, *142*, 144501. [CrossRef]
26. Mirsaleh-Kohan, N.; Fischer, A.; Graves, B.; Bolorizadeh, M.; Kondepudi, D.; Compton, R.N. Laser Shock Wave Induced Crystallization. *Cryst. Growth Des.* **2017**, *17*, 576–581. [CrossRef]
27. Kacker, R.; Dhingra, S.; Irimia, D.; Ghatkesar, M.K.; Stankiewicz, A.; Kramer, H.J.M.; Eral, H.B. Multiparameter Investigation of Laser-Induced Nucleation of Supersaturated Aqueous KCl Solutions. *Cryst. Growth Des.* **2018**, *18*, 312–317. [CrossRef]
28. del Río-Sancho, S.; Pan Delgado, D.; de la Fuente, G.F.; García-Caballero, T.; Taboada-Suárez, A.; Csaba, N.; Bao-Varela, C.; José Alonso, M. Laser-Induced Transient Skin Disruption to Enhance Cutaneous Drug Delivery. *Eur. J. Pharm. Biopharm.* **2020**, *156*, 165–175. [CrossRef] [PubMed]
29. McGinney, J.A. Redetermination of the Structures of Potassium Sulphate and Potassium Chromate: The Effect of Electrostatic Crystal Forces upon Observed Bond Lengths. *Acta Cryst. B* **1972**, *28*, 2845–2852. [CrossRef]
30. Arnold, H.; Kurtz, W.; Richter-Zinnius, A.; Bethke, J.; Heger, G. The Phase Transition of K_2SO_4 at about 850 K. *Acta Crystallogr. Sect. B* **1981**, *37*, 1643–1651. [CrossRef]
31. Mydlarz, J.; Jones, A.G. Potassium Sulfate Water-Alcohols Systems: Composition and Density of Saturated Solutions. *J. Chem. Eng. Data* **1990**, *35*, 214–216. [CrossRef]
32. Mydlarz, J.; Jones, A.G.; Millan, A. Solubility and Density Isotherms for Potassium Sulfate-Water-2-Propanol. *J. Chem. Eng. Data* **1989**, *34*, 124–126. [CrossRef]
33. Polyanskiy, M.N. Refractive Index Database. Available online: <https://refractiveindex.info>. (accessed on 15 July 2021).
34. Jiang, S.; ter Horst, J.H. Crystal Nucleation Rates from Probability Distributions of Induction Times. *Cryst. Growth Des.* **2011**, *11*, 256–261. [CrossRef]
35. Hua, T.; Gawayed, O.; Grey-Stewart, D.; Garetz, B.A.; Hartman, R.L. Microfluidic Laser-Induced Nucleation of Supersaturated Aqueous KCl Solutions. *Cryst. Growth Des.* **2019**, *19*, 3491–3497. [CrossRef]
36. Matviiv, R.B.; Rudysh, M.Y.; Stadnyk, V.Y.; Fedorchuk, A.O.; Shchepanskyi, P.A.; Brezvin, R.S.; Khyzhun, O.Y. Structure, Refractive and Electronic Properties of K_2SO_4 : Cu^{2+} (3%) Crystals. *Curr. Appl. Phys.* **2021**, *21*, 80–88. [CrossRef]
37. Wilhelm, E.; Battino, R.; Wilcock, R.J. Low-Pressure Solubility of Gases in Liquid Water. *Chem. Rev.* **1977**, *77*, 219–262. [CrossRef]
38. Lee, J.I.; Yim, B.-S.; Kim, J.-M. Effect of Dissolved-Gas Concentration on Bulk Nanobubbles Generation Using Ultrasonication. *Sci. Rep.* **2020**, *10*, 18816. [CrossRef]